Biochemical and Biophysical Research Communications 435 (2013) 367–372

Contents lists available at SciVerse ScienceDirect

Biochemical and Biophysical Research Communications

journal homepage: www.elsevier.com/locate/ybbrc

Crystal structure of GTPase-activating domain from human MgcRacGAP

Atsushi Matsuura [a], Hyung Ho Lee [a,b,*]

[a] Department of Bio & Nano Chemistry, Kookmin University, Seoul 136-702, Republic of Korea
[b] Department of Integrative Biomedical Science and Engineering, Kookmin University, Seoul 136-702, Republic of Korea

ARTICLE INFO

Article history:
Received 16 April 2013
Available online 7 May 2013

Keywords:
MgcRacGAP
GTPase activating protein
Cytokinesis
Rac1

ABSTRACT

Cytokinesis in animal cells relies on a centralspindlin complex consisting of male germ cell RacGap (MgcRacGAP) and mitotic kinesin-like protein 1 (MKLP1). Rho GTPases act as molecular switches to regulate the actin cytoskeleton for cytokinesis, of which Rac1 is regulated by MgcRacGAP. In this study, we determined the crystal structure of the GTPase-activating protein (GAP) domain of MgcRacGAP at a resolution of 1.9 Å. The conformation of Arg385, which is a key residue for GAP activity, was found to be different from that of previously reported GAP proteins, and MgcRacGAP (residues 348–546) was found to exist as a monomer in solution, according to Stokes radii. We also measured the GAP activity of MgcRacGAP mutants for Rac1.

1. Introduction

The final step of cell division is cytokinesis, wherein 2 daughter cells are produced from a single cell. The assembly of the central spindle during anaphase in animal cells directs contractile ring constriction and cleavage furrow formation through the Rho family of GTPases and its regulators [1]. The Rho family of GTPases and its effectors mediate spindle signaling during anaphase [2]. GTPase-activating proteins (GAPs) inactivate GTPases by stimulating intrinsic GTPase activity, while guanine nucleotide-exchange factors (GEFs) activate GTPases by promoting the exchange of GDP for GTP [3]. GTPase activity is maintained by a balance of local GTPase inactivation by GAPs and local GTPase activation by GEFs [3].

Rho GTPases act as molecular switches to regulate the actin cytoskeleton; 3 common members of the Rho family are RhoA, Rac1, and Cdc42 [3]. Centralspindlin, which consists of mitotic kinesin-like protein 1 (MKLP1), which is a Rho GTPase activating protein (Rho-GAP), and male germ cell RacGap (MgcRacGAP), plays an essential role in the assembly of the central spindle in cytokinesis [4,5]. The N-terminus of MgcRacGAP interacts with MKLP1 by forming a coiled coil, and the C-terminus of MgcRacGAP contains GAP activity for RhoA-family GTPases [6]. MgcRacGAP localizes precisely to the central spindle and functions as an important regulator to recruit other cytokinetic regulators [7]. MgcRacGAP stimulates the intrinsic GTPase activities of Rac1 and Cdc42, but not that of RhoA [8]. However, MgcRacGAP is functionally changed into a RhoA GAP by Ser387 phosphorylation mediated by Aurora B kinase [9]. Moreover, the GAP activity of MgcRacGAP is down-regulated by PRC1 binding, and it contributes to Cdc42 activation and mitotic spindle formation [10]. CYK-4 (the MgcRacGAP homolog from *Caenorhabditis elegans*) stimulates GTP hydrolysis of Cdc42 and the Rac1 homolog (Rac), but it has little effect on RhoA [11]. In parallel with the activation of RhoA by Ect-2 (RhoGEF), inactivation of Rac by CYK-4 functions to drive cytokinesis [12].

The crystal structures of several small GTPases, GAPs, and their complexes have been previously reported. In the crystal structure of p50rhoGAP, Arg85 and Asn194 are important in binding to RhoA (or Cdc42 GTPase) and enhancing GTPase activity [13–15]. The crystal structure of human Cdc42 (GMPPNP, the non-hydrolysable GTP analog) in complex with the GAP domain of p50rhoGAP showed that Cdc42 makes contact with a shallow pocket on the GAP domain through its switch I and II regions [14]. A conformational change (rotation of 20° between the Rho and GAP domains) was observed in the crystal structure of the RhoA-p50rhoGAP complex (GDP and AlF_4, the transition-state analog) when the complex structure was compared with the Cdc42 (GMPPNP bound)-p50rhoGAP complex [15]. The crystal structures of the Cdc42 (GDP and AlF4)-p50rhoGAP and Cdc42 (GDP and AlF_4)-p50rhoGAP (R305A mutant) complexes showed that an arginine residue on the A–A′ loop is important to stabilize the transition state of the GTPase reaction [16]. Position 95 of GTPase (Glu95 of Cdc42, Glu97 of RhoA, and Ala95 of Rac1) is an important determinant of binding specificity between GTPases and GrafGAP on the basis of structural and mutational studies of the GAP domain of the *Gallus gallus*

Abbreviations: MgcRacGAP, male germ cell RacGap; MKLP1, mitotic kinesin-like protein 1; GAPs, GTPase-activating proteins; GEFs, guanine nucleotide exchange factors; GST, glutathione S-transferase; TEV, tobacco etch virus; IPTG, isopropyl-β-D-1-thiogalactopyranoside; PMSF, phenylmethylsulfonyl fluoride.

* Corresponding author at: Department of Bio & Nano Chemistry, Kookmin University, Seoul 136-702, Republic of Korea. Fax: +82 2 910 4415.
E-mail address: hhlee@kookmin.ac.kr (H.H. Lee).

0006-291X/$ - see front matter © 2013 Elsevier Inc. All rights reserved.
http://dx.doi.org/10.1016/j.bbrc.2013.04.094

GTPase regulator associated with focal adhesion kinase (Graf) [17]. The structure-based model of the Rac-specific GAP domain of β2-chimaerin suggested that Phe315 and Glu317 in the A′ helix interact with Ala88 and Ala95 of Rac1, which are key determinants of contact with Rac1 [18]. In spite of the number of structural studies conducted so far, the structure of human MgcRacGAP remains uncharacterized. To provide further insight into the structure of MgcRacGAP, we report the crystal structure of the GAP domain of human MgcRacGAP. The GAP activity assay and mutational studies on MgcRacGAP provide molecular insight into how MgcRacGAP activates Rac1 to regulate cytokinesis.

2. Materials and methods

2.1. Protein preparation

Human cDNA clones encoding MgcRacGAP (clone ID: hMU005205) and Rac1 (clone ID: KU000510) were purchased from the 21C Frontier Human Gene Bank (http://genbank.kribb.re.kr). The GAP domain of human MgcRacGAP (amino acids 348–546, MgcRacGAP$_{348–546}$) was cloned into the parallel vector pGST2 [19] and expressed in *Escherichia coli* strain BL21(DE3) cells as a fusion protein with an N-terminal GST (glutathione S-transferase) tag followed by a TEV protease cleavage site. The MgcRacGAP$_{348–546}$ was induced with 0.5 mM isopropyl-β-D-1-thiogalactopyranoside (IPTG) and expressed at 25 °C for 16 h. Cells were lysed by passing them through a French press in a lysis buffer containing 20 mM Tris–HCl (pH 8.0), 200 mM NaCl, 5 mM 2-mercaptoethanol, 1 mM phenylmethylsulfonyl fluoride (PMSF), and 5% (w/v) glycerol. Protein was purified using an affinity column on Glutathione Sepharose 4B (GE Healthcare) and cleaved with TEV protease. The MgcRacGAP$_{348–546}$ was further purified by size exclusion chromatography (HiLoad 16/600 Superdex 200 prep grade, GE Healthcare) and concentrated to 10 mg/ml by ultrafiltration. The R385A and N495A mutations of MgcRacGAP$_{348–546}$ were introduced by site-directed mutagenesis by using a Quikchange™ kit (Stratagene). The MgcRacGAP$_{348–546}$ mutants (R385A and N495A) were expressed and purified in the same manner as the wild-type MgcRacGAP$_{348–546}$. Full-length human Rac1 (amino acids 1–192) was cloned and expressed in the same way as human MgcRacGAP$_{348–546}$. Cells were lysed by passing them through a French press in 20 mM Tris–HCl pH 8.0, 200 mM NaCl, 5 mM 2-mercaptoethanol, 1 mM PMSF, and 5% (w/v) glycerol. Protein was purified using a Glutathione Sepharose 4B affinity column and by size exclusion chromatography (HiLoad 16/600 Superdex 200) without removing the GST-tag.

2.2. Crystallization, structure determination, and refinement

Crystals of human MgcRacGAP$_{348–546}$ were grown at 298 K using the sitting drop method by mixing 1 μl of a 10 mg/ml solution of MgcRacGAP$_{348–546}$ in 20 mM Tris–HCl (pH 8.0), 200 mM NaCl, and 1 mM dithiothreitol with 1 μl of reservoir solution consisting of 100 mM sodium cacodylate buffer (pH 5.7) and 13% polyethylene glycol 6000. The crystals were transferred to a solution containing the reservoir solution and 25% glycerol for cryoprotection. Data was collected at 100 K in 1° oscillations at the 7A beamline of the Pohang Light Source (Pohang Accelerator Laboratory).

Crystals of MgcRacGAP$_{348–546}$ diffracted to a resolution of 1.9 Å, and the diffraction data were processed and scaled using the *HKL2000* software package [20]. The crystal belonged to space group $P2_12_12_1$, with unit cell parameters of $a = 41.47$ Å, $b = 63.16$ Å, and $c = 74.08$ Å. The structure was solved using the molecular replacement method using human p50rhoGAP model (PDB ID: 1RGP) as a probe. A cross-rotational search followed by a translational search was performed using the *PHASER* program [21]. Subsequent manual model building was performed using the *COOT* program [22] and restrained refinement was carried out using the *REFMAC5* program [23]. Several rounds of model building, simulated annealing, positional refinement, and individual *B*-factor refinement were performed using the *COOT* and *REFMAC5* programs. Table 1 lists the refinement statistics. The atomic coordinates and structure factors were deposited in the Protein Data Bank (accession codes 3W6R).

2.3. Analytical gel filtration

Purified MgcRacGAP$_{348–546}$ was subjected to analytical gel filtration chromatography on a Superdex 200 (10/300 GL) column with a running buffer (20 mM Tris–HCl pH 8.0 and 200 mM NaCl) at a constant flow rate of 0.5 ml/min. The standard curve was obtained using molecular weight markers (Sigma). The Stokes radii of β-amylase, alcohol dehydrogenase, carbonic anhydrase, and cytochrome C were calculated from the crystal structures of each protein (PDB codes: 1FA2, 2HCY, 1V9E, and 1HRC, respectively) by using the *HYDROPRO* program [24].

2.4. GAP activity assay

Purified GST-Rac1 and MgcRacGAP$_{348–546}$ (or its mutants) were mixed to obtain a concentration of 10 μM each in 20 mM Tris–HCl buffer (pH 8.0) containing 200 mM NaCl, 10 μM $MgCl_2$, and 1 mM GTP (guanosine 5-triphosphate, Sigma) and incubated for 30 min at 22 °C. As a control, the other reaction components were run without introducing MgcRacGAP$_{348–546}$ into the reaction tube. GTP hydrolysis was monitored by measuring the production of inorganic phosphate at 660 nm using an acidic ammonium molybdate solution (ammonium molybdate tetrahydrate, Sigma) with malachite green oxalate (Sigma) [25]. Standard curves produced using known amounts of phosphate (KH_2PO_4, Sigma) were linear and highly consistent.

Table 1
Statistics for data collection and refinement.

Data set	MgcRacGAP348-546
A. Data collection statistics	
X-ray source	BL-7A (Pohang Light Source)
X-ray wavelength (Å)	0.97928
Space group	P212121
a, *b*, *c* (Å)	41.47, 63.16, 74.08
Resolution range (Å)	50–1.9
Total/unique reflections	93,141/15,787
Completeness (%)	99.2 (98.3)[a]
Average $I/\sigma(I)$	51.6 (5.2)[a]
R_{merge}[b] (%)	8.5 (48.5)[a]
B. Model refinement statistics	
Resolution range (Å)	25.3–1.9
R_{work}/R_{free}[c] (%)	22.1/25.9
Number/average B-factor (Å^2)	
Protein nonhydrogen atoms	1584/22.4
Water oxygen atoms	133/26.6
R.m.s. deviations from ideal	
Bond lengths (Å)	0.005
Bond angles (°)	0.94
Protein-geometry analysis	
Ramachandran favored (%)	96.46
Ramachandran allowed (%)	3.54
Ramachandran outliers (%)	0

[a] Values in parentheses refer to the highest resolution shell (1.93–1.90 Å).

[b] $R_{merge} = \sum_{hkl}\sum_i|I_i(hkl) - \langle I(hkl)\rangle|/\sum_{hkl}\sum_i I_i(hkl)_i$, where $I(hkl)$ is the intensity of reflection *hkl*, $\sum_{hkl}$ is the sum over all reflections, and $\sum_i$ is the sum over *i* measurements of reflection *hkl*.

[c] $R = \sum_{hkl}||F_{obs}| - |F_{calc}||/\sum_{hkl}|F_{obs}|$, where R_{free} was calculated for a randomly chosen 5% of reflections, which were not used for structure refinement and R_{work} was calculated for the remaining.

3. Results and discussion

3.1. Crystal structure determination of human MgcRacGAP$_{348–546}$

The crystal structure of MgcRacGAP$_{348–546}$ was determined by the molecular replacement method using human p50rhoGAP model (PDB ID: 1RGP) at a resolution of 1.9 Å (Fig. 1A and B). The refined models gave R_{work}/R_{free} values of 22.1/25.9 for 25.3–1.9 Å (Table 1). The refined model of MgcRacGAP$_{348–546}$ accounts for residues 348–546 with a cloning artifact (Met347) in an asymmetric unit with 133 water molecules. Ramachandran plot analysis of the refined model showed that 96.46%, 3.54%, and 0% of the non-glycine residues were in the most favored regions, allowed regions, and disallowed regions, respectively (Table 1). The crystal structure of MgcRacGAP$_{348–546}$ primarily consists of 11 helices (9 α-helices and two 3_{10} helices), of which the 9 α-helices have been labeled from A to G′ (Fig. 1B). To analyze the quaternary structure of MgcRacGAP$_{348–546}$ in solution, analytical gel filtration was performed using a Superdex 200 (10/300 GL) column (Fig. 1C and D). The Stokes radius of MgcRacGAP$_{348–546}$ was estimated to be 2.50 nm, which is highly similar to the calculated Stokes radius (2.43 nm) of the MgcRacGAP$_{348–546}$ monomer. This result suggests that MgcRacGAP$_{348–546}$ exists as a monomer in solution.

3.2. Overall structure and structural comparisons

The overall structure of MgcRacGAP$_{348–546}$ is similar to those of the GAP domains of other Rho GTPase-activating proteins (RhoGAPs) (Fig. 2A) [17,18]. A structural similarity search for MgcRacGAP$_{348–546}$ using the DALI server [26] identified several crystal structures of RhoGAPs. When the structure of MgcRacGAP$_{348–546}$ was overlapped with those of the other RhoGAPs (p50RhoGAP, N-chimaerin, DLC1, and p190RhoGAP), the r.m.s. deviations were 0.73 Å, 0.60 Å, 1.00 Å, and 0.95 Å for the 109, 124, 105, and 123 Cα atoms, respectively. Although the overall structure was similar to that of other RhoGAPs, significant structural differences were observed in several helices of MgcRacGAP$_{348–546}$ (Fig. 2A and B). When distance plots between MgcRacGAP$_{348–546}$ and the corresponding Cα positions of the GAP domains were drawn as a function of residue number, the differences between MgcRacGAP$_{348–546}$ and other GAP domains (p50RhoGAP, N-chimaerin, DLC1, and p190RhoGAP) were found to be significant (~5 Å) on helices A′, C, and G (with average B-factors of 37.1, 18.1, and 17.1 Å^2, respectively; Fig. 2B). Arg385 in human MgcRacGAP, a strictly conserved residue in many GAP domains, is a key residue both in the interaction with a small GTPase and a transition-state stabilization during GTP hydrolysis [15]. The Arg385 of MgcRacGAP adopts a conformation that differs from that of other RhoGAPs (Fig. 2C and D), whereas another key residue, Asn495, adopts a conformation similar to those of other RhoGAPs (Fig. 2C). The average B-factors of Arg385 and Asn495 are sufficiently low (28.9 and 22.4 Å^2, respectively) to suggest a rigid conformation. Furthermore, Arg385 is exposed in a solvent channel in the crystal, without interacting closely with neighboring MgcRacGAP$_{348–546}$ molecules, which indicates that the unique conformation of Arg385 is not a crystallographic artifact.

3.3. Structural insights into Rac1 recognition of MgcRacGAP$_{348–546}$

To obtain information on the mode of binding between MgcRacGAP$_{348–546}$ and its substrate, Rac1, we tried to build a

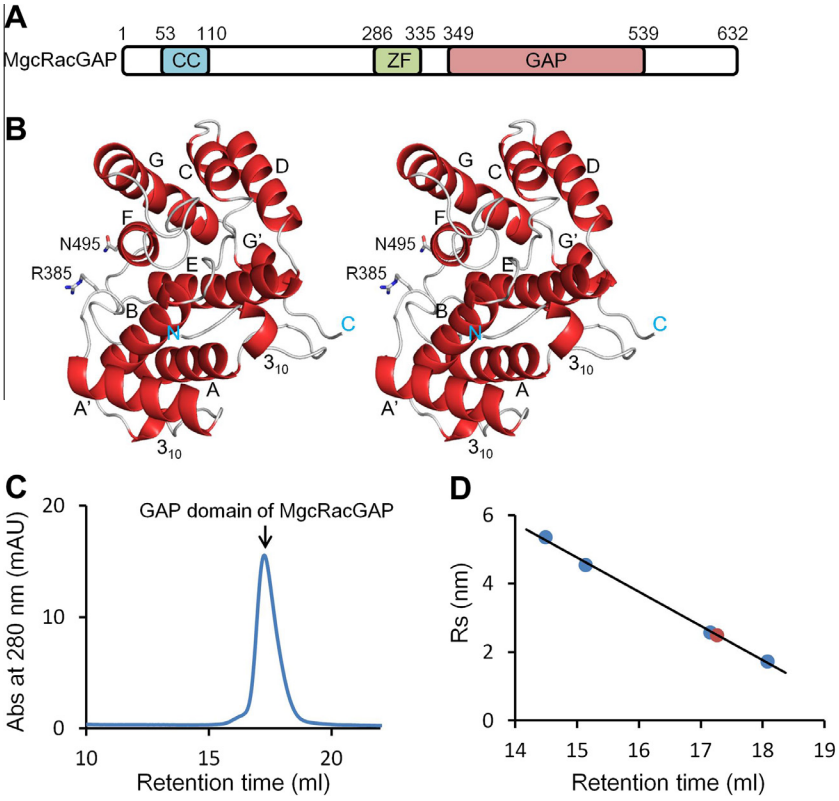

Fig. 1. Architecture of human MgcRacGAP. (A) MgcRacGAP domain architecture, including the coiled-coil region (CC), the zinc finger region (ZF), and the GTPase-activating domain (GAP). (B) Stereo ribbon diagram of MgcRacGAP$_{348–546}$. Helices are colored in red. All figures, including protein structures, were drawn using PyMOL software (The PyMOL Molecular Graphics System, http://www.pymol.org). (C) Analytical gel filtration profile of MgcRacGAP$_{348–546}$. (D) Standard curve using molecular weight markers. The positions of the molecular weight markers (β-amylase, alcohol dehydrogenase, carbonic anhydrase, and cytochrome C) are indicated in blue dots, respectively. The position of MgcRacGAP$_{348–546}$ is marked with a red dot. (For interpretation of the references to color in this figure legend, the reader is referred to the web version of this article.)

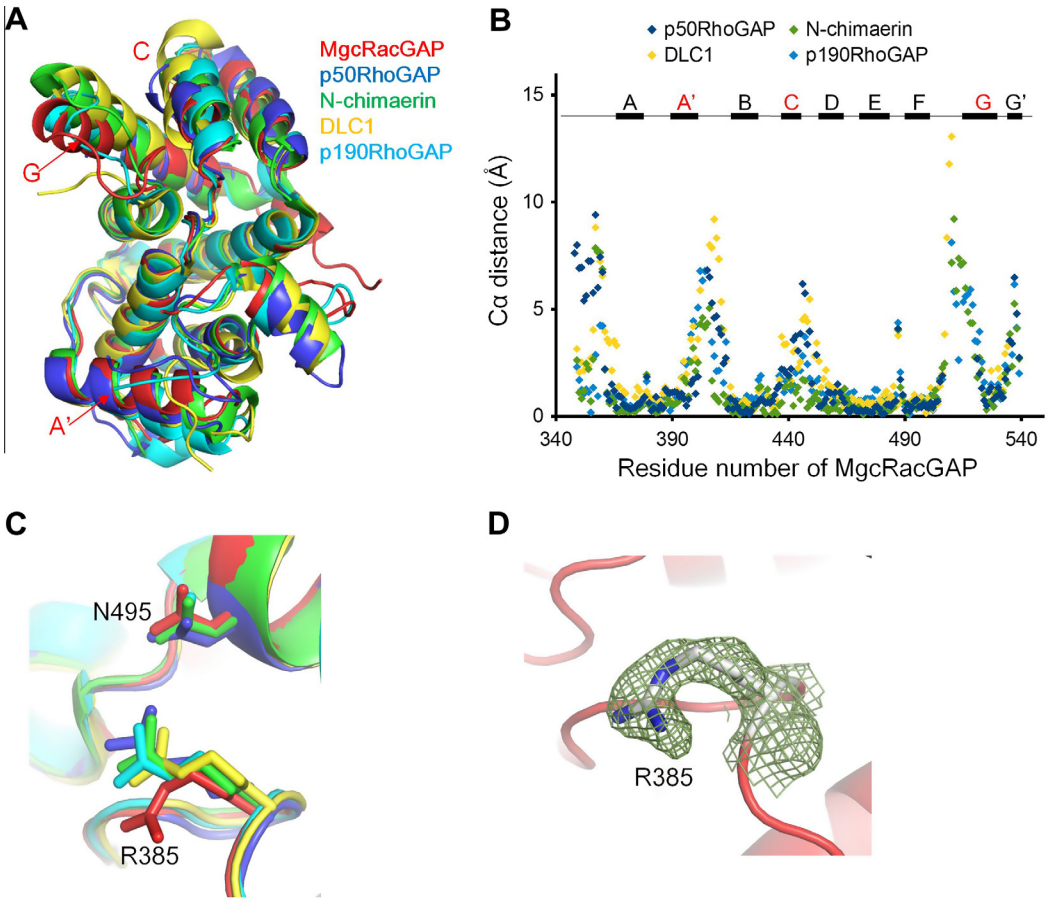

Fig. 2. Structural comparisons of the GAP domains. (A) Superposition of MgcRacGAP$_{348-546}$ (PDB ID 3W6R, colored in red) with that of p50RhoGAP (PDB ID 1RGP, colored in blue), N-chimaerin (PDB ID 2OSA, colored in green), DLC1 (PDB ID 3KUQ, colored in yellow), and p190RhoGAP (PDB ID 3FK2, colored in cyan). (B) Distance plots between MgcRacGAP$_{348-546}$ and the corresponding Cα positions of the GAP domains (p50RhoGAP colored in blue, N-chimaerin colored in green, DLC1 colored in yellow, and p190RhoGAP colored in cyan). Rectangles above the plots represent the α-helical structure of MgcRacGAP$_{348-546}$. The α-helices that are structurally different between MgcRacGAP$_{348-546}$ and other GAP domains are labeled in red. (C) The side chains of Arg385 and Asn495 of MgcRacGAP$_{348-546}$ (colored in red) and the equivalent residues of p50RhoGAP (Arg282 and Asn391, colored in blue), N-chimaerin (Arg304 and Asn417, colored in green), DLC1 (Arg1114 and Asn1224, colored in yellow), and p190RhoGAP (Arg1284 and Asn1395, colored in cyan) are superimposed and shown as sticks. (D) Electron density for the side chain of Arg385 of MgcRacGAP$_{348-546}$ (1.0 sigma). (For interpretation of the references to color in this figure legend, the reader is referred to the web version of this article.)

model on the basis of previously determined structures of complexes between RhoGAPs and small GTPases. Some structures of complexes between human RhoGAPs and small GTPases (RhoA and Cdc42) have also been previously reported [14–16] (Fig. 3A). Crystal structures of complexes between GAP domains and small GTPases were structurally superimposed by overlapping the GAP domains of each complex (Fig. 3A). Subsequently, MgcRacGAP$_{348-546}$ was superimposed over the corresponding GAP domains of each complex, whereas Rac1 was superimposed over the RhoA protein of the p50RhoGAP-RhoA complex (Fig. 3A). Thus, a composite model of the MgcRacGAP$_{348-546}$–Rac1 complex was produced (Figs. 3A and 4A). When MgcRacGAP$_{348-546}$ was overlapped with the RhoGAP domain of RhoGAP-small GTPase complexes (p50RhoGAP-RhoA, p50RhoGAP-Cdc42, and ArhGAP20-RhoA), the r.m.s. deviations were 0.79 Å, 0.72 Å, and 1.21 Å for the 114, 108, and 117 Cα atoms, respectively, suggesting that the complexes were similar in their folding, although there are some deviations in several helices, as observed by the superposition of GAP domains of the RhoGAP structures (Figs. 2A and 3A).

MgcRacGAP$_{348-546}$ and other RhoGAPs adopt the same folding, with a small GTPase binding pocket formed in several helices (B and F) and loops between A–A′ and F–G (Fig. 3A). When the surface diagram around the expected binding surface obtained from the complex model of MgcRacGAP$_{348-546}$ and Rac1 was examined, several residues (Arg385, Ser387, Lys423, Met491, Asn495, and Pro502) that are strictly conserved among eukaryotic RhoGAPs were found to be clustered, suggesting their significance in the recognition of Rac1 (Fig. 3B). Fig. 3B shows an image obtained by a ~90° rotation of MgcRacGAP$_{348-546}$ relative to the orientation of the image shown in Fig. 3A. When the molecular surface is colored according to its electrostatic potential, the charge distributions differ significantly among MgcRacGAP$_{348-546}$, p50RhoGAP, and ArhGAP20, suggesting that the charge distribution contributes to specific interactions between RhoGAPs and the corresponding small GTPases (Fig. 3C). Interestingly, the surface charges between MgcRacGAP$_{348-546}$ and Rac1 are complementary (positively charged on the surface of MgcRacGAP$_{348-546}$ and negatively charged on the surface of Rac1, enclosed in dotted green circles in Fig. 3C), suggesting that the charge-charge interactions contribute to formation of the complex between the 2 proteins.

As the Arg385 of MgcRacGAP adopts a conformation that differs from those of other RhoGAPs, we attempted to verify whether Arg385 is properly positioned in the composite model of the MgcRacGAP$_{348-546}$–Rac1 complex (Fig. 4A). The distances between the oxygen atoms (O2A and O2B) in the diphosphate group of GDP and the nitrogen atom in the guanidino group of Arg305 in p50RhoGAP are 2.9 (2.9) Å and 2.9 (2.6) Å, respectively, in the p50RhoGAP-RhoA(Cdc42) complex, suggesting that close contact is important

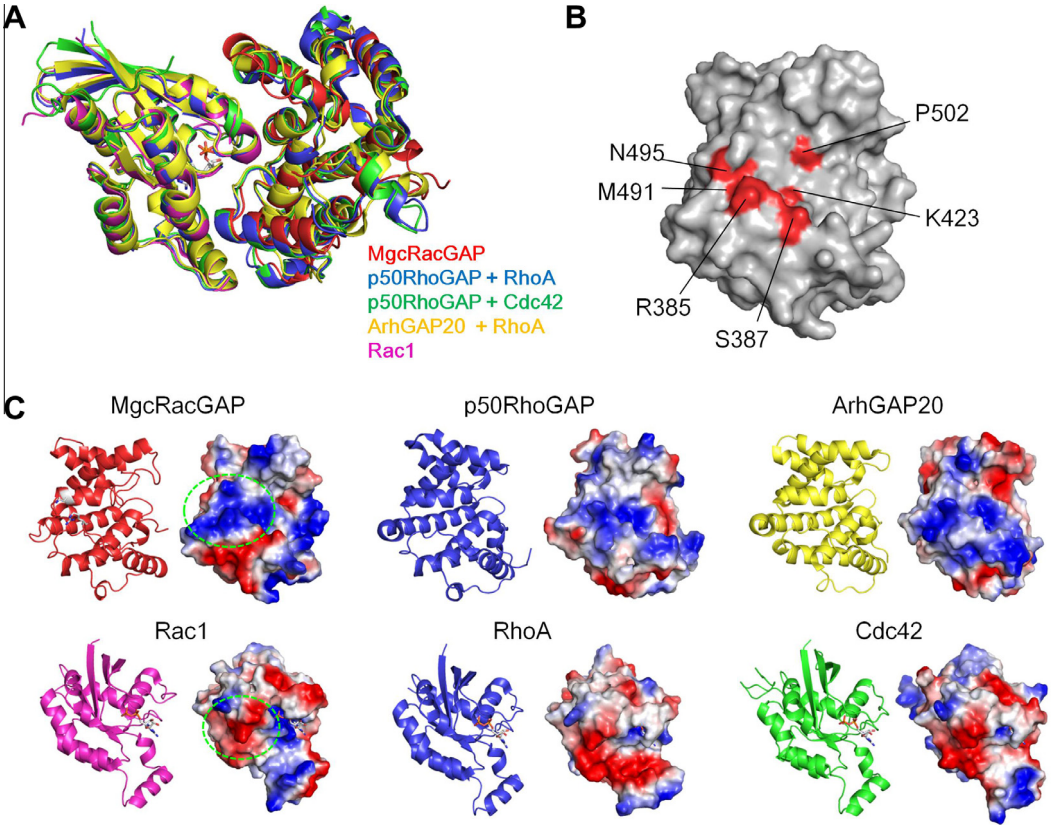

Fig. 3. Structural comparisons of the GAP domains in complex with small GTPases. (A) Superposition of the structure of $MgcRacGAP_{348–546}$ (PDB ID 3W6R, colored in red) with those of the p50RhoGAP-RhoA complex (PDB ID 1TX4, colored in blue), p50RhoGAP-Cdc42 complex (PDB ID 1GRN, colored in green), ArhGAP20-RhoA complex (PDB ID 3MSX, colored in yellow), and Rac1 (PDB ID 1G4U, colored in magenta). Complexes of the GAP domains and a small GTPase were structurally superimposed by overlapping $MgcRacGAP_{348–546}$ with the corresponding GAP domains. Rac1 was superimposed over the RhoA molecule of the p50RhoGAP-RhoA complex. (B) Sequence conservation mapped onto the surface of $MgcRacGAP_{348–546}$ (identical residues are colored in red). (C) Ribbon model and electrostatic potential on the surfaces of the interfaces between GAP domains and small GTPases. (For interpretation of the references to color in this figure legend, the reader is referred to the web version of this article.)

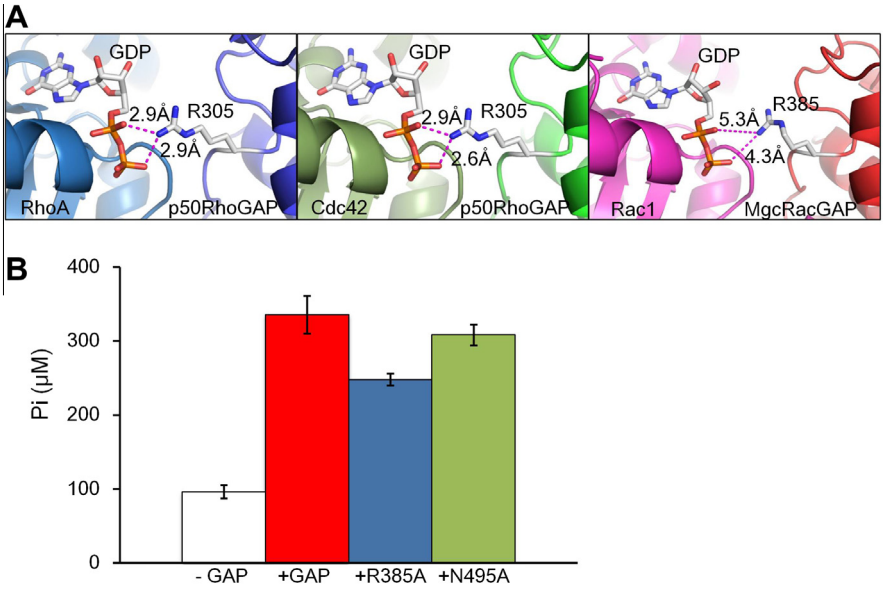

Fig. 4. Structural comparison of RhoGAP-GTPase complexes around Arg385 and GAP activity assay. (A) Molecular interactions between the GDP molecules of GTPases (RhoA, Cdc42, and Rac1) and the Arg residues of the RhoGAPs (Arg305 in p50RhoGAP and R385 in MgcRacGAP). Different proteins are drawn in different colors. Red dotted lines denote hydrogen bonds. (B) Purified GST-Rac1 and $MgcRacGAP_{348–546}$ (or its mutants), and GTP were mixed to estimate the stimulation of GTP hydrolysis by $MgcRacGAP_{348–546}$. Error bars indicate a standard deviation for quintuplicate samples. (For interpretation of the references to color in this figure legend, the reader is referred to the web version of this article.)

for the GAP activity of RhoGAPs (Fig. 4A). In the $MgcRacGAP_{348–546}$–Rac1 model, however, the corresponding distances are significantly larger (5.3 and 4.3 Å) because of the different conformation of Arg385 (Fig. 4A). This finding suggests that $MgcRacGAP_{348–546}$ and Rac1 form a complex with a binding mode different from that of other RhoGAP-GTPase complexes.

3.4. GAP activity of MgcRacGAP toward Rac1

To confirm that MgcRacGAP$_{348-546}$ displays GAP activity *in vitro*, human Rac1 (amino acids 1–192) was expressed in *E. coli*. Previous studies showed that full-length MgcRacGAP and MgcRacGAP$_{238-513}$ exhibit GAP activities toward Cdc42 and Rac1 but are less active on RhoA [8,27]. In our study, we used more truncated MgcRacGAP$_{348-546}$ and examined its GAP activity toward the Rac1 GTPase by measuring the concentration of inorganic phosphate (P_i) released from the GTP molecule. The amount of P_i produced by the incubation of MgcRacGAP$_{348-546}$ and Rac1 in a GTP-containing buffer was found to be significantly higher (~3.5 times) than that of a control that omitted MgcRacGAP$_{348-546}$ without adding magnesium ions (Fig. 4B), suggesting that a metal ion had been incorporated into Rac1 during the purification steps. The R385A and N495A mutants exhibited a diminished GTP hydrolytic activity (35% and 10% of wild-type levels, respectively), which supports the importance of the 2 residues for its activity.

Acknowledgments

The authors thank the staff at Beamline 7A of the Pohang Light Source for their assistance during the X-ray experiments. This study was supported by a National Research Foundation of Korea grant funded by the Korean government (MEST; Grant No. 2012K1A3A1A09033383 and 2012-0004058) to HHL.

References

[1] M. Glotzer, The molecular requirements for cytokinesis, Science 307 (2005) 1735–1739.
[2] K. Kamijo, N. Ohara, M. Abe, T. Uchimura, H. Hosoya, J.-S. Lee, T. Miki, Dissecting the role of Rho-mediated signaling in contractile ring formation, Mol. Biol. Cell 17 (2006) 43–55.
[3] W.M. Bement, A.L. Miller, G. von Dassow, Rho GTPase activity zones and transient contractile arrays, BioEssays 28 (2006) 983–993.
[4] E.A. White, M. Glotzer, Centralspindlin: at the heart of cytokinesis, Cytoskeleton 69 (2012) 882–892.
[5] K. Hirose, T. Kawashima, I. Iwamoto, T. Nosaka, T. Kitamura, MgcRacGAP is involved in cytokinesis through associating with mitotic Spindle and midbody, J. Biol. Chem. 276 (2001) 5821–5828.
[6] V. Pavicic-Kaltenbrunner, M. Mishima, M. Glotzer, Cooperative assembly of CYK-4/MgcRacGAP and ZEN-4/MKLP1 to form the centralspindlin complex, Mol. Biol. Cell 18 (2007) 4992–5003.
[7] W.M. Zhao, G. Fang, MgcRacGAP controls the assembly of the contractile ring and the initiation of cytokinesis, Proc. Natl. Acad. Sci. USA 102 (2005) 13158–13163.
[8] A. Touré, O. Dorseuil, L. Morin, P. Timmons, B. Jégou, L. Reibel, G. Gacon, MgcRacGAP, a new human GTPase-activating protein for Rac and Cdc42 Similar to drosophila rotundRacGAP gene product, is expressed in male germ cells, J. Biol. Chem. 273 (1998) 6019–6023.
[9] Y. Minoshima, T. Kawashima, K. Hirose, Y. Tonozuka, A. Kawajiri, Y.C. Bao, X. Deng, M. Tatsuka, S. Narumiya, W.S. May Jr., T. Nosaka, K. Semba, T. Inoue, T. Satoh, M. Inagaki, T. Kitamura, Phosphorylation by aurora B converts MgcRacGAP to a RhoGAP during cytokinesis, Dev. Cell 4 (2003) 549–560.
[10] R. Ban, Y. Irino, K. Fukami, H. Tanaka, Human mitotic spindle-associated protein PRC1 inhibits MgcRacGAP activity toward Cdc42 during the metaphase, J. Biol. Chem. 279 (2004) 16394–16402.
[11] V. Jantsch-Plunger, P. Gönczy, A. Romano, H. Schnabel, D. Hamill, R. Schnabel, A.A. Hyman, M. Glotzer, CYK-4: a Rho family GTPase activating protein (GAP) required for central spindle formation and cytokinesis, J. Cell Biol. 149 (2000) 1391–1404.
[12] J.C. Canman, L. Lewellyn, K. Laband, S.J. Smerdon, A. Desai, B. Bowerman, K. Oegema, Inhibition of Rac by the GAP activity of centralspindlin is essential for cytokinesis, Science 322 (2008) 1543–1546.
[13] T. Barrett, B. Xiao, E.J. Dodson, G. Dodson, S.B. Ludbrook, K. Nurmahomed, S.J. Gamblin, A. Musacchio, S.J. Smerdon, J.F. Eccleston, The structure of the GTPase-activating domain from p50rhoGAP, Nature 385 (1997) 458–461.
[14] K. Rittinger, P.A. Walker, J.F. Eccleston, K. Nurmahomed, D. Owen, E. Laue, S.J. Gamblin, S.J. Smerdon, Crystal structure of a small G protein in complex with the GTPase-activating protein rhoGAP, Nature 388 (1997) 693–697.
[15] L. Rittinger, P.A. Walker, J.F. Eccleston, S.J. Smerdon, S.J. Gamblin, Structure at 1.65Å of RhoA and its GTPase-activating protein in complex with a transition-state analogue, Nature 389 (1997) 758–762.
[16] N. Nassar, G.R. Hoffman, D. Manor, J.C. Clardy, R.A. Cerione, Structures of Cdc42 bound to the active and catalytically compromised forms of Cdc42GAP, Nat. Struct. Biol. 5 (1998) 1047–1052.
[17] K.L. Longenecker, B. Zhang, U. Derewenda, P.J. Sheffield, Z. Dauter, J.T. Parsons, Y. Zheng, Z.S. Derewenda, Structure of the BH domain from graf and its implications for Rho GTPase recognition, J. Biol. Chem. 275 (2000) 38605–38610.
[18] B. Canagarajah, F.C. Leskow, J.Y. Ho, H. Mischak, L.F. Saidi, M.G. Kazanietz, J.H. Hurley, Structural mechanism for lipid activation of the Rac-specific GAP, β2-chimaerin, Cell 119 (2004) 407–418.
[19] P. Sheffield, S. Garrard, Z. Derewenda, Overcoming expression and purification problems of RhoGDI using a family of "parallel" expression vectors, Protein Expr. Purif. 15 (1999) 34–39.
[20] Z. Otwinowski, W. Minor, Processing of X-ray diffraction data collected in oscillation mode, Methods Enzymol. 276 (1997) 307–326.
[21] A.J. McCoy, R.W. Grosse-Kunstleve, P.D. Adams, M.D. Winn, L.C. Storoni, R.J. Read, Phaser crystallographic software, J. Appl. Cryst. 40 (2007) 658–674.
[22] P. Emsley, K. Cowtan, Coot: model-building tools for molecular graphics, Acta Cryst. D 60 (2004) 2126–2132.
[23] G.N. Murshudov, A.A. Vagin, E.J. Dodson, Refinement of macromolecular structures by the maximum-likelihood method, Acta Cryst. D 53 (1997) 240–255.
[24] J. García de la Torre, M.L. Huertas, B. Carrasco, Calculation of hydrodynamic properties of globular proteins from their atomic-level structure, Biophys. J. 78 (2000) 719–730.
[25] P.A. Lanzetta, L.J. Alvarez, P.S. Reinach, O.A. Candia, An improved assay for nanomole amounts of inorganic phosphate, Anal. Biochem. 100 (1979) 95–97.
[26] L. Holm, P. Rosenström, Dali server: conservation mapping in 3D, Nucleic Acid Res. 38 (2010) W545–549.
[27] T. Kawashima, K. Hirose, T. Satoh, A. Kaneko, Y. Ikeda, Y. Kaziro, T. Nosaka, T. Kitamura, MgcRacGAP is involved in the control of growth and differentiation of hematopoietic cells, Blood 96 (2000) 2116–2124.